J|A|C|S
ARTICLES
Published on Web 03/19/2003

Interfacial Electron Transfer in $Fe^{II}(CN)_6^{4-}$−Sensitized TiO_2 Nanoparticles: A Study of Direct Charge Injection by Electroabsorption Spectroscopy

Mikhail Khoudiakov, Alejandro R. Parise,† and Bruce S. Brunschwig*,‡

Contribution from the Department of Chemistry, Brookhaven National Laboratory, P.O. Box 5000, Upton, New York, 11973-5000

Received December 30, 2002; E-mail: BSB@BNL.GOV

Abstract: Electroabsorption (Stark) spectroscopy has been used to study the dye sensitized interfacial electron transfer in an $Fe^{II}(CN)_6^{4-}$ donor complex bound to a TiO_2 nanoparticle. The average charge-transfer distance determined from the Stark spectra is 5.3 Å. This value is similar to the estimated distance between the Fe^{II} center of the complex and the Ti^{IV} surface site coordinated to the nitrogen end of a bridging CN ligand in $(CN)_5Fe^{II}-CN-Ti^{IV}$(particle). This finding suggests that the electron injection is to either an individual titanium surface site or a small number of Ti centers localized around the point of ferrocyanide coordination to the particle and not into a conduction band orbital delocalized over the nanoparticle. The polarizability change, $Tr(\Delta\alpha)$, between the ground and the excited states of the $Fe^{II}(CN)_6^{4-}-TiO_2$(particle) system is ~3 time larger than normally observed in mixed-valence dinuclear metal complexes. It is proposed that the large polarizability of the excited state increases the dipole-moment changes measured by Stark spectroscopy.

Introduction

Interfacial electron transfer between adsorbed molecular species and semiconductor nanoparticles has been a subject of intense research in recent years.[1] Dye-sensitized TiO_2 nanoparticles and films are one of the most studied systems primarily because of their important application in liquid junction photovoltaic cells.[2,3] Two types of dye sensitization have been reported. One involves the direct injection of an electron from the dye to the nanoparticle.[4,5] The second occurs through indirect injection: an excited state of the dye molecule is initially formed that then transfers an electron to the particle.[6,7] The direct injection mechanism gives rise to a new charge-transfer absorption band that is observed when the dye is attached to the particle, whereas no new absorption features are present in the indirect mechanism. For the direct mechanism, the charge transfer (CT) is essentially instantaneous and takes place during the absorption process.[8] The initially formed Franck−Condon state has a hole on the dye and an extra electron on the nanoparticle. The indirect mechanism of charge injection has also been shown to be very fast.[9] The back electron transfer from the reduced nanoparticle to the oxidized dye following either type of injection occurs on a much slower time scale and is generally nonexponential.[10] To account for this and other observations it has been proposed that a variety of trap sites exists on the particles.

TiO_2 nanoparticles and $Fe^{II}(CN)_6^{4-}$ ions are known to form charge-transfer complexes at low pH,[3,11,12] as indicated by the formation of a new absorption band at ~420 nm (Figure 1). The iron complex is believed to bind at a surface Ti^{IV} site via a monodentate cyanide ligand, $(CN)_5Fe^{II}-CN-Ti^{IV}$(particle), as shown in Figure 1 (inset), and this structure is supported by IR[8] and resonance Raman[13] studies. The 420 nm absorption band has been assigned as a metal-to-particle charge-transfer (MPCT) transition.[5,12−15] In the $Fe^{II}(CN)_6^{4-}-TiO_2$(particle) complexes excitation of the charge-transfer band leads to injection of electrons into TiO_2 and the formation of $Fe^{III}(CN)_6^{3-}$.[3,11,12] The forward electron injection occurs in less than 50 fs.[8] The very

† Current address: Department of Inorganic, Analytical, and Physical Chemistry, Faculty of Exact and Natural Sciences, University of Buenos Aires, (C1428EHA) Buenos Aires, Argentina.

‡ Current address: Beckman Institute, California Institute of Technology, Mail Code 139−74, 1200 East California Blvd., Pasadena, CA 91125, BSB@caltech.edu.

(1) Miller, R. J. D.; McLendon, G. L.; Nozik, A. J.; Schmickler, W.; Willing, F. *Surface Electron-Transfer Processes*; Wiley-VCH: New York, 1995.
(2) O'Regan, B.; Grätzel, M. *Nature* **1991**, 737−739.
(3) Nazeeruddin, M. K.; Kay, A.; Rodicio, I.; Humphrybaker, R.; Muller, E.; Liska, P.; Vlachopoulos, N.; Grätzel, M. *J. Am. Chem. Soc.* **1993**, *115*, 6382−6390.
(4) Weng, Y. X.; Wang, Y. Q.; Asbury, J. B.; Ghosh, H. N.; Lian, T. Q. *J. Phys. Chem. B* **2000**, *104*, 93−104.
(5) Yang, M.; Thompson, D. W.; Meyer, G. J. *Inorg. Chem.* **2000**, *39*, 3738−3739.
(6) Ferrere, S.; Gregg, B. A. *J. Am. Chem. Soc.* **1998**, *120*, 843−844.
(7) Moser, J. E.; Grätzel, M. *Chimia* **1998**, *52*, 160−162.
(8) Ghosh, H. N.; Asbury, J. B.; Weng, Y.; Lian, T. *J. Phys. Chem. B* **1998**, *102*, 10 208−10 215.
(9) Hannappel, T.; Burfeindt, B.; Storck, W.; Willig, W. *J. Phys. Chem. B* **1997**, *101*, 6799−6802.
(10) Gaal, D. A.; Hupp, J. T. *J. Am. Chem. Soc.* **2000**, *122*, 10 956−10 963.
(11) Lu, H.; Prieskorn, J. N.; Hupp, J. T. *J. Am. Chem. Soc.* **1993**, *115*, 4927−4928.
(12) Vrachnou, E.; Vlachopoulos, N.; Grätzel, M. *Chem. Commun.* **1987**, 868−870.
(13) Blackbourn, R. L.; Johnson, C. S.; Hupp, J. T. *J. Am. Chem. Soc.* **1991**, *113*, 1060−1062.
(14) Vrachnou, G.; Grätzel, M.; McEvou, A. J. *J. Electroanal. Chem.* **1989**, 193−205.
(15) Doorn, S. K.; Blackbourn, R. L.; Johnson, C. S.; Hupp, J. T. *Electrochim. Acta* **1991**, *36*, 1775−1785.

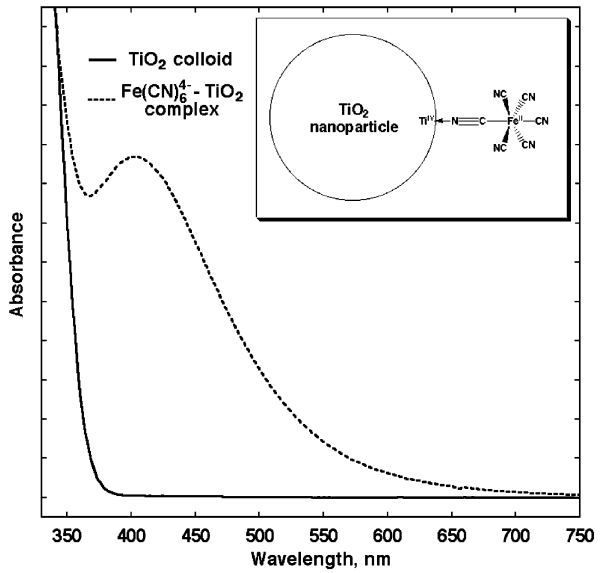

Figure 1. UV−vis spectra of 2 nm TiO_2 nanoparticles in 50:50 water/ethylene glycol (solid line) and the resulting $Fe^{II}(CN)_6^{4-}$−TiO_2(particle) system (dotted line) at 298 K.

rapid injection together with the formation of a new CT absorption band supports the hypothesis that the optical absorption involves direct electron transfer to the TiO_2 nanoparticle.[16] The standard model for electron injection into a nanoparticle maintains that the electron initially enters the conduction band and then is trapped by local sites within the particle. Unfortunately, the observed spectroscopic signature of the electron within a TiO_2 nanoparticle has not been assigned to either a trapped or a free electron.[8]

Electroabsorption (Stark) spectroscopy affords a unique way of characterizing the initially formed charge-transfer state; providing information on the distance of the initial charge transfer and the changes in the dipole moment and polarizability between the ground and Franck−Condon state. For the direct injection mechanism, this should elucidate whether in the Franck−Condon state the electron is in a delocalized conduction band state of the particle or rather localized on an individual titanium center. There has been one report on the application of Stark emission spectroscopy to interfacial electron-transfer process: Hupp and co-workers studied TiO_2-eosin Y and TiO_2-coumarin 343 complexes in PVA films.[17] In this paper, we report the first Stark absorption spectra of a dye attached to a free nanoparticle in solution. For comparison, we also investigated a mixed-valence polymeric Fe^{II}−Ti^{IV} cyanide complex.

Experimental Section

All chemicals were obtained from Aldrich and used as received. Ultrapure deionized water (18.2 MΩ) was prepared with a Millipore Milli-Q system. The size of TiO_2 nanoparticles was determined using a Precision Detectors dynamic light scattering instrument. Anatase particles were also characterized by transmission electron microscopy (JEOL 100CX2 instrument, 100 keV accelerating voltage), and X-ray synchrotron powder diffraction (data were collected at the ×7B beamline of the National Synchrotron Light Source, Brookhaven National Laboratory). Ultrafiltration was performed using Amicon YM10 membranes (10 kD MW cutoff). Indium tin oxide (ITO) coated glass (2 cm × 2.5 cm × 0.1 cm, 250 Å coating) was obtained from Cargo Limited. Kapton film (25 or 50 μm) was obtained from Dupont.

Preparation of Anatase TiO_2 Nanoparticles ($D_h \approx 5$ nm). An adaptation of previously published synthetic methods was used.[4,18] Titanium(IV) isopropoxide (0.9 mL) was dissolved in 9 mL of anhydrous 2-propanol. The resulting solution was added dropwise (0.1 mL/min, controlled by a syringe pump) to 100 mL of water acidified to a pH of 1.30 with HNO_3 at 1 °C under vigorous stirring. The colloid was stirred at 1 °C for 48 h to narrow the size distribution. To produce a sample suitable for Stark spectroscopy the colloid was mixed with 100 mL of ethylene glycol and concentrated by ultrafiltration to the final volume of ≈5 mL.

Preparation of Amorphous TiO_2 Nanoparticles ($D_h \approx 2$ nm). Titanium(IV) isopropoxide (4 mL) was dissolved in 10 mL of anhydrous 2-propanol. The resulting solution was rapidly (<1 min) added to a mixture containing 10 mL of water, 10 mL of ethylene glycol, and 2 mL of concentrated HCl under vigorous stirring (white precipitate formed and quickly redissolved). After 30 min of stirring the volatiles were removed by rotary evaporation under vacuum at 40−50 °C. The residue was dissolved in 10 mL of 0.5 M HCl producing a clear colloid solution that was stable for months at room temperature.

Preparation of Amorphous TiO_2 Nanoparticles ($D_h \approx 6$, 10, and 21 nm). Titanium(IV) isopropoxide (2 mL) was dissolved in 50 mL of anhydrous ethylene glycol. The solution was heated to 140 (6 nm), 160 (10 nm), or 180 (21 nm) °C and equilibrated at this temperature (the mixture turns milky white). Water (2 mL) was injected under vigorous stirring (the solution becomes clear again). The mixture was removed from heat after 1 h, allowed to cool to room temperature, and mixed with 50 mL of 0.5 M HCl. The colloid was concentrated by ultrafiltration to the final volume of ∼10 mL.

Preparation of $Fe^{II}(CN)_6^{4-}$−TiO_2(particle) Complexes. TiO_2 colloids (0.7 M TiO_2, 0.25 M HCl (0.025 M HNO_3 for anatase particles), 50:50 water/ethylene glycol) were mixed with 25 mM $K_4Fe(CN)_6$ solution in 50:50 water/ethylene glycol in the following proportions:

TiO_2 colloid mL	$K_4Fe(CN)_6$ solution mL	size (D_h) nm
1.0	1.0	2
1.0	0.4	5[a]
1.0	0.5	6
1.0	0.4	10
1.0	0.3	21

[a] Anatase TiO_2 nanoparticles

The mixture was vigorously shaken and ultrasonicated briefly producing a dark brown solution stable for a few days (unlike aqueous colloids, $Fe^{II}(CN)_6^{4-}$ binding to TiO_2 in 50:50 water/ethylene glycol is not affected by oxygen). It should be noted that TiO_2 colloids of larger particles (5−21 nm) gel readily upon addition of $K_4Fe(CN)_6$. To avoid this, the $K_4Fe(CN)_6$ solution was added in aliquots of 0.1 mL.

Preparation of a Polymeric Mixed-Valence Fe^{II}−Ti^{IV} Cyanide Complex. The complex was prepared according to previously published procedures.[14,19] Solutions of $TiCl_3$ (154 mg in 10 mL of deaerated 3 M HCl) and $K_3Fe(CN)_6$ (329 mg in 10 mL of deaerated water) were loaded into syringes and rapidly mixed under argon. The brown gel precipitate was ultrasonicated for 10 min, separated by centrifugation (55 000 g, 20 min), and washed with 10 mL of water (10 min of ultrasonic treatment followed by centrifugation). To prepare a sample for Stark spectroscopy, the complex was dispersed in 10 mL of water by ultrasonic treatment (10 min). Large particulates were removed by centrifugation (55 000 g, 20 min) and the supernatant was mixed with

(16) Yang, M.; Thompson, D. W.; Meyer, G. J. *Inorg. Chem.* **2002**, *41*, 1254−1262.
(17) Walters, K. A.; Gaal, D. A.; Hupp, J. T. *J. Phys. Chem. B* **2002**, *106*, 5139−5143.
(18) Colombo, D. P.; Roussel, K. A.; Saeh, J.; Skinner, D. E.; Cavaleri, J. J.; Bowman, R. M. *Chem. Phys. Lett.* **1995**, *232*, 207−214.
(19) Maer, K.; Beasley, M. L.; Collins, R. L.; Milligan, W. O. *J. Am. Chem. Soc.* **1968**, *90*, 3201−3208.

10 mL of ethylene glycol. Alternatively, the complex can be prepared by starting with equal volumes of 0.1 M $TiCl_4$ solution in 3 M HCl and 0.1 M aqueous $K_4Fe(CN)_6$ solution and following the same procedure. According to our dynamic light scattering studies, the complex does not have any appreciable molecular solubility in water, but is solubilized in the form of colloidal particles with a size ranging from 20 to 300 nm.

Stark Measurements. The electroabsorption apparatus and experimental procedures were as previously reported.[20,21] Briefly, the sample cell was constructed from two pieces of ITO glass with the coated surfaces facing one another. A 1.5 × 2 cm piece of Kapton film with a rectangular cutout in the center was used as a spacer. A drop of sample solution passed through a 0.45 μm Millipore filter was placed on the coated side of the ITO glass with Kapton spacer and then covered with the other ITO piece, placed in a staggered position to leave space for electrical connections. Two spring-loaded clamps were used to hold the pieces in place. The sample was placed in a liquid-nitrogen immersion Dewar with optical windows and an AC electric field ($6-8 \times 10^6$ V/m) was applied. The electroabsorption component of the transmitted light (horizontally polarized) was resolved by a lock-in amplifier (SR830, Stanford Research System), tuned to twice the frequency of the modulation of the electrical field. The electroabsorption spectrum for each complex was measured a minimum of three times and the fit parameters presented are the average values with each sample examined at $\chi = 90°$ and 55°, where χ is the angle between the applied electric field and the plane of polarization of the light. As expected for a system of rigid randomly oriented dipoles, the intensity of the Stark signal was proportional to the square of the external electric field.

Data Treatment. The data analysis was carried out as previously described[20,21] by using the zeroth, first and second derivatives of the absorption spectrum to fit the electroabsorption $\Delta\epsilon(\nu)/\nu$ spectrum, in terms of the Liptay treatment[22]

$$\Delta\epsilon(\nu)/\nu = \left[A_x\epsilon(\nu)/\nu + \frac{B_x}{15h}\frac{\partial(\epsilon(\nu)/\nu)}{\partial\nu} + \frac{C_x}{30h^2}\frac{\partial^2(\epsilon(\nu)/\nu)}{\partial\nu^2}\right]\boldsymbol{F}_{\mathrm{int}}{}^2 \quad (1)$$

where ν is the frequency of the light in Hz. For a fixed randomly oriented sample, the following relationships hold for all the coefficients A_x, B_x, and C_x

$$C_x = C_1 + (3\cos^2(\chi) - 1)C_2 \quad (2)$$

The dipole-moment change for the charge-transfer excitation is obtained from the coefficient of the second derivative term

$$|\Delta\boldsymbol{\mu}_{12}| = \sqrt{C_1/5} \quad (3)$$

$$|\boldsymbol{m}\cdot\Delta\boldsymbol{\mu}_{12}| = \sqrt{C_2/3 + C_1/15} \quad (4)$$

where $\boldsymbol{m}$ is the unit transition dipole moment, $\boldsymbol{m}_{12}/|\boldsymbol{m}_{12}|$. The polarizability change can be related approximately to the coefficient of the first derivative term

$$\mathrm{Tr}(\Delta\boldsymbol{\alpha}) = \frac{2}{3}B_1 \quad (5)$$

$$\boldsymbol{m}\cdot\Delta\boldsymbol{\alpha}\cdot\boldsymbol{m} = \frac{2}{3}\left(B_2 + \frac{1}{2}B_1\right) \quad (6)$$

The internal electric field is related to the applied external field by $\mathbf{F}_{\mathrm{int}} = f_{\mathrm{int}}\mathbf{F}_{\mathrm{ext}}$. For the water/ethylene glycol medium used here the local field correction f_{int} is estimated as 1.33.[20]

Molecular Modeling. Molecular modeling was done using Cerius2 (version 4.2) software from Accelrys. The Cerius2 software contains modules for doing molecular mechanics and DFT calculations. The molecular mechanics calculations were done using the universal force field[23,24] that contains parameters for metal atoms. DFT calculations were done using Dmol3[25,26] revision 99.1101. DFT calculations were performed on the structure optimized using molecular mechanics with the universal force field. Spectra are approximated by the differences in orbital energies.

Results and Discussion

Synthesis of TiO_2 Nanoparticles. We have developed two novel procedures for preparing nanoscale TiO_2 utilizing ethylene glycol as a solvent. The hydrothermal synthesis is similar to the route recently reported by Feldmann and Jungk for the synthesis of various oxide nanoparticles in diethylene glycol with sizes ranging from 50 to 200 nm.[27] Using ethylene glycol affords smaller particles with the size tunable in the 5−30 nm range (Figure 2a−c).

The size is controlled primarily by the temperature of the reaction mixture, although changes in the Ti(i-OPr)$_4$/H_2O ratio and reaction time also have some effect. According to the X-ray powder diffraction data, the TiO_2 nanoparticles prepared at 140 and 160 °C were amorphous. The sample prepared at 180 °C showed some degree of crystallinity (anatase), but was also largely amorphous. Unfortunately, due to inherent low contrast of titanium oxide and the amorphous nature of the nanoparticles, we were unable to obtain any TEM images of the samples prepared by the hydrothermal procedure. However, for anatase TiO_2 nanoparticles prepared by low-temperature hydrolysis we found dynamic light scattering data to be in good agreement with transmission electron microscopy and X-ray powder diffraction results: $D_h = 5 \pm 1.5$ nm (DLS), $D = 4 \pm 1$ nm (TEM), $D_c = 3.5$ nm (powder diffraction, Scherrer's formula).

The second procedure involves rapid hydrolysis of 2-propanol solution of Ti(i-OPr)$_4$ in strongly acidic water/ethylene glycol mixture. The resulting amorphous nanoparticles are ultra-small ($D_h \approx 2$ nm) and have a narrow size distribution (Figure 2d). It should be noted that TiO_2 nanocolloids prepared by both methods are extremely stable and can be stored at room temperature for months.

$Fe^{II}(CN)_6{}^{4-}$−TiO_2(particle) Complexes. $Fe^{II}(CN)_6{}^{4-}$−TiO_2(particle) complexes were synthesized using nanoparticles having diameters from 2 to 20 nm. In all cases the complexes have a new absorption band at 420 nm (Figure 1). No other absorptions at lower energy are observed from 500 to 2300 nm. The assignment of the 420 nm absorption in the $Fe^{II}(CN)_6{}^{4-}$−TiO_2(particle) complexes to an Fe^{II} to Ti^{IV} charge-transfer transition is somewhat surprising.[16] The energy of the charge-transfer band can be estimated from: $h\nu = \Delta G° + \lambda$, where $\Delta G°$ is the free-energy difference between $(CN)_5Fe^{II}$−CN−Ti^{IV}(particle) and $(CN)_5Fe^{III}$−CN−Ti^{III}(particle) and λ is the reorganization energy for the MPCT transition. $\Delta G° = E^{Fe} - E^{Ti} + \Delta G_b$, where E^{Ti} and E^{Fe} are the flatband potential of the

(20) Shin, Y.-G.; Brunschwig, B. S.; Creutz, C.; Sutin, N. *J. Phys. Chem.* **1996**, *100*, 8157−8169.
(21) Coe, B. J.; Harris, J. A.; Brunschwig, B. S. *J. Phys. Chem. A* **2002**, *106*, 897−908.
(22) Liptay, W. In *Excited States*; Lim, E. C., Ed.; Academic Press: New York, 1974; Vol. 1, pp 129−229.
(23) Castonguay, L. A.; Rappe, A. K. *J. Am. Chem. Soc.* **1992**, *114*, 5832−5842.
(24) Rappe, A. K.; Colwell, K. S.; Casewit, C. J. *Inorg. Chem.* **1993**, *32*, 3438−3450.
(25) Delley, B. *J. Chem. Phys.* **1990**, *92*, 508−517.
(26) Delley, B. *J. Chem. Phys.* **1991**, *94*, 7245−7250.
(27) Feldmann, C.; Jungk, H. O. *Angew. Chem.-Int. Edit.* **2001**, *40*, 359−362.

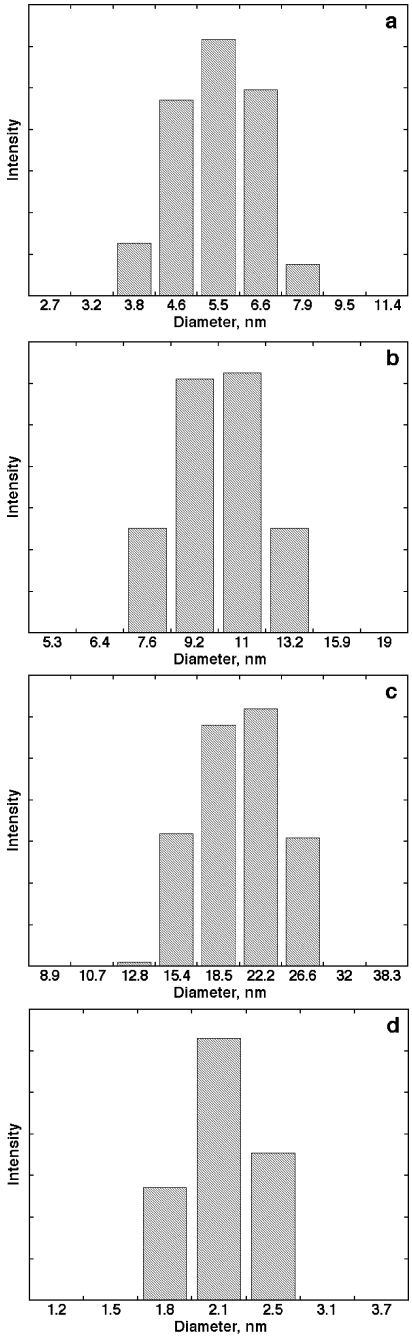

Figure 2. Size distribution of TiO_2 nanoparticles obtained by the hydrothermal procedure at 140 °C ($D_h = 5.6$ nm) panel (a), 160 °C ($D_h = 10.2$ nm) panel (b), 180 °C ($D_h = 20.5$ nm) panel (c), and by hydrolysis in strongly acidic water/ethylene glycol mixture ($D_h = 2.2$ nm) panel (d).

TiO_2 (particle) and the reduction potential of the $Fe(CN)_6^{3-}$, respectively; and $\Delta G_b = RT \ln(K^{II}/K^{III})$, where K^{II} and K^{III} are the binding constants for the $Fe(CN)_6^{4-}$ and $Fe(CN)_6^{3-}$ to the titanium surface, respectively. If we assume[16] that the binding of the $Fe(CN)_6^{4-}$ is 10^2 to 10^5 more favorable than the binding of the $Fe(CN)_6^{3-}$, the reorganization energy is less than 1 eV,[16,28] and using potentials for the TiO_2 (pH $\approx$ 2) and $Fe(CN)_6^{3-}$ of ~ -0.36[29] and ~ 0.4[13,28,30] V, respectively, we obtain $h\nu < 2.1$ eV or $\lambda_{max} > 590$ nm. This suggests one of the following: that the injection is into a state well above the edge of the conduction band, that there is significant inner shell reorganization energy associated with the titanium center or that the observed transition does not involve injection of an iron electron. For comparison, in our model dinuclear complex, $[(CN)_5Fe-CN-Ti(H_2O)_4O]^{2-}$, the titanium potential is better approximated by the value for Ti^{IV} ion in solution, which is significantly more positive at $\approx$0.131 eV. This yields an absorption wavelength of $\approx$800 nm. Preliminary DFT calculations on the $[(CN)_5Fe-CN-Ti(H_2O)_4O]^{2-}$ complex predict strong CT absorptions at $\sim$900 and $\sim$300 nm that involve charge transfer from the filled Fe *d* orbitals to the empty Ti *d* orbitals and from the π orbitals of the axial and equatorial CN^- groups to the same Ti d orbitals, respectively.

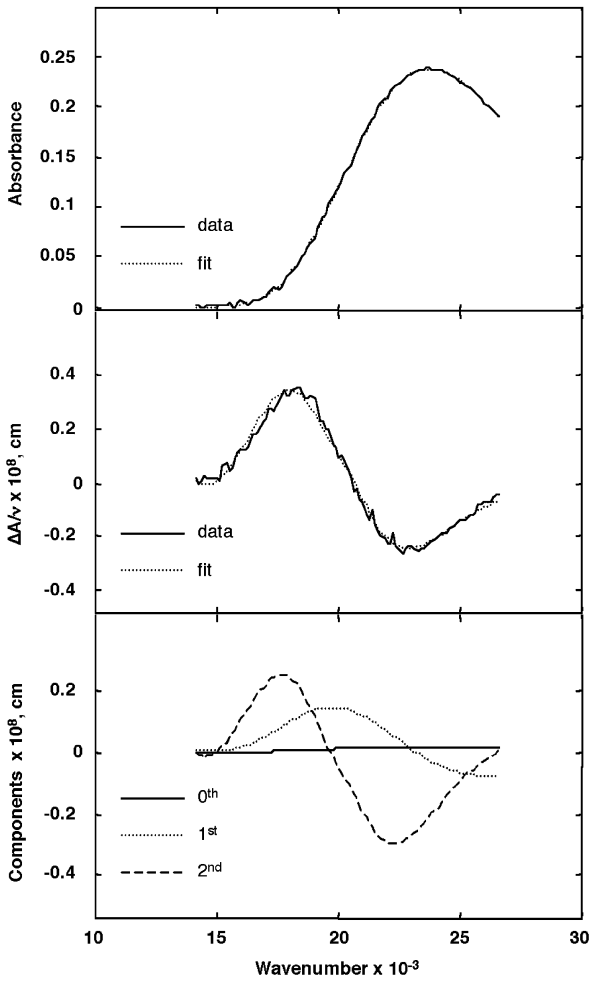

Figure 3. Representative absorption, electroabsorption spectra and electroabsorption spectral components of $Fe^{II}(CN)_6^{4-}$−sensitized TiO_2 nanoparticles at 77 K in a 50:50 water/ethylene glycol glass. Top panel: absorption spectrum, experimental data (solid line) and fit (dotted line); middle panel: electroabsorption spectrum, experimental data (solid line) and fit (dotted line) according to Liptay equation; bottom panel: contribution of 0^{th} (solid line), 1st (dotted line), and 2nd (dashed line) derivatives of the absorption spectrum to the calculated fit.

Stark Spectroscopy. Representative MPCT absorption and electroabsorption spectra and electroabsorption spectral components of $Fe^{II}(CN)_6^{4-}-TiO_2$(particle) are shown in Figure 3.

As for many $Ru^{III}(NH_3)_5L$ complexes (L = aromatic N-heterocycle),[20,21] the electroabsorption spectra can be modeled in terms of a large second-derivative term, a small first-derivative component, and a negligible zeroth-derivative com-

(28) Hupp, J. T.; Williams, R. D. *Acc. Chem. Res.* **2001**, *34*, 808−817.
(29) Yan, S. G.; Hupp, J. T. *J. Phys. Chem.* **1996**, *100*, 6867−6870.
(30) Sutin, N. In *Bioinorganic Chemistry II*; Raymond, K. N., Ed.; American Chemical Society: Washington, DC, 1977; Vol. 162, pp 156−172.

Table 1. Summary of Spectral Data and Stark Fitting Results

D nm	$h\nu_{max,77\,K}$ $cm^{-1}\times10^3$	$\|\boldsymbol{\mu}_{12}\|$ eÅ	$\|\Delta\boldsymbol{\mu}_{12}\|^a$ eÅ	$\|\Delta\boldsymbol{\mu}_{ab}\|^a$ EÅ	$H_{ab}{}^b$ $cm^{-1}\times10^3$	$Tr(\Delta\alpha)^c$ Å^3	$c_b{}^{2\,d}$
2	25.1	0.80	4.7	4.9	4.1	500	0.03
5[e]	23.2	0.88	5.5	5.8	3.5	900	0.02
6	23.8	0.87	5.0	5.3	4.0	800	0.03
10	23.9	0.82	5.6	5.8	3.3	800	0.02
21	24.0	0.80	5.7	6.0	3.2	900	0.02
$Fe^{II}-Ti^{IV}$[f]	26.0	0.57	3.6	3.8	3.0	300	0.02

[a] The estimated uncertainties of $|\Delta\boldsymbol{\mu}|$ values are ±15%. [b] Electronic coupling element between the charge-transfer centers. [c] Polarizability change between the ground and excited states (±50% uncertainty). [d] Degree of delocalization between the charge-transfer centers. [e] Anatase TiO_2 nanoparticles. [f] Mixed-valence polymeric $Fe^{II}-Ti^{IV}$ cyanide complex.

ponent contribution. Parameters resulting from fitting the spectra to the Liptay equation are summarized in Table 1. For all the particles the $|\Delta\boldsymbol{\mu}_{12}|$ values are similar, ranging from 4.7 to 5.7 eÅ. Within experimental error, the angle between the transition dipole moment and the change in dipole-moment vectors did not differ from zero (a near zero value would be expected if the vectors were collinear along the $Fe^{II}-NC-Ti^{IV}$ axis). Although the uncertainty of experimental results (±15%) does not permit reliable conclusions, it appears that for amorphous particles the dipole-moment change increases by 20% as the particle size increases (2, 6, 10, and 21 nm particles). Also, for particles of roughly the same size the dipole-moment change is larger for crystalline TiO_2 (5 nm anatase vs 6 nm amorphous particles).

It has been pointed out[32−34] that the relationship between a second-derivative line shape and a dipole-moment change breaks down when there are a number of overlapping bands and the shifts in the absorptions due to the electric field are small compared with the spectral width of the transitions. One example is the Stark spectroscopy of CdSe nanoparticles. In these studies, no dye is present and the band gap absorption is probed. Although it was found that the Stark ensemble absorption spectra could be fit with a large second derivative contribution,[35,36] it was argued that the (second-derivative) line shape was due to the superposition of contributions due to the changes in polarizability from multiple bands.[32,33] The emission Stark spectra of single CdSe nanocrystallites have also been studied;[34] it was found that the polarizability of the emitting state was much larger than that of the ground state by $\sim10^5$ Å^3 and that individual particles would at times exhibit large dipole moments in their excited state. The authors argue that this dipole moment is induced by local electric fields produced by charge carriers on or near the surface of the particle. These transient fields polarize the delocalized excited state and when they are correctly oriented result in very large observed dipole-moment changes of ~18 eÅ, yielding an effective charge-transfer distance equal to the size of the particle (the hole and electron are located on opposite sides of the particle). These dipole-moment changes are averaged to zero in the ensemble absorbance measurements.[33,35,36]

If one assumes that the second-derivative line shape observed in this work is at least partially due to large polarizability changes coupled to overlapping bands, then the actual dipole-moment change is smaller that the Liptay analysis yields and a very small charge-transfer distance is implicated. The polarizability changes in the CdSe systems are 2 orders of magnitude larger than we obtain from our fitting of the Stark spectra. If polarizabilities as large as 10^5 Å are present in the excited state, one would expect a delocalized electron on the particle to be strongly polarized by the charge on the dye (we note that one unit of charge located 2 Å from a 20 Å nanoparticle would produce a delocalized field of $>10^8$ V/m at the center of the particle and with a polarizability of 10^5 Å^3 would give a dipole moment of 200 eÅ!). This would lead to a very large contribution to the dipole-moment change, which is in contradiction to our above assumption.

Thus the second derivative line shape observed here are best interpreted as due to dipole-moment changes between the ground and excited states. The dipole-moment changes yield an average charge-transfer distance ($R_{12} = |\Delta\boldsymbol{\mu}_{12}|/e^-$) of 5.3 Å. This value is close to the $Fe^{II}-Ti^{IV}$ distance of 5.1−5.3 Å estimated from the molecular modeling of $[(CN)_5Fe-CN-Ti(H_2O)_4O]^{2-}$. In all cases the charge-transfer distances observed for $Fe^{II}(CN)_6{}^{4-}-TiO_2$(particles) are much shorter than one would expect if the electron were transferred from the iron to an orbital delocalized over the whole particle (10 to 100 Å). This finding suggests that the direct charge injection is from the iron center to an orbital primarily residing on one or a few titanium centers that are very close to the point of attachment of the $Fe(CN)_6{}^{4-}$ moiety and not into a delocalized conduction band state. If the band at 420 nm is due to ligand-to-metal charge transfer from the nonbridging CN^-'s to a Ti^{IV} atom on the surface of the nanoparticles, then the observed charge-transfer distance of 5.3 Å is slightly shorter than the average nonbridging CN^- to Ti^{IV} distance. This is also consistent with direct charge injection into an orbital localized on the surface rather than delocalized over the particle.

INDO calculations[37] have suggested that in the catechol−TiO_2 (particle) system the directly injected electron goes into an orbital that has a significant contribution from the Ti 3d orbital closest to the adsorbate with some additional contributions from other adjacent Ti centers. In addition, nonadiabatic molecular dynamics simulations[38] on indirect injection from isonicotinic acid into TiO_2 nanoparticles show that for this system the acceptor state is delocalized over only several Ti atoms extending radially from the point of attachment for about three lattice layers into the particle. If for the $Fe^{II}(CN)_6{}^{4-}-TiO_2$(particles) system studied here we assume that the electron is transferred from an Fe centered orbital to an orbital delocalized over a few Ti atoms that extend into the particle for about three layers, we would expect a charge-transfer distance of ~6.5 Å. This distance is consistent with our observed value of ~5.3 Å assuming that the Stark-derived distance is shorter than the nominal center-to-center separation of the donor and acceptor orbitals as seen in dinuclear systems (see below).

When Stark spectroscopy is applied to molecular systems, one generally observes charge-transfer distances that are shorter

(31) Brunschwig, B. S.; Sutin, N. *Inorg. Chem.* **1979**, *18*, 1731−1736.
(32) Dabbousi, B. O.; Bawendi, M. G.; Onitsuka, O.; Rubner, M. F. *Appl. Phys. Lett.* **1995**, *66*, 1316−1318.
(33) Sacra, A.; Norris, D. J.; Murray, C. B.; Bawendi, M. G. *J. Chem. Phys.* **1995**, *103*, 5236−5245.
(34) Empedocles, S. A.; Bawendi, M. G. *Science* **1997**, *278*, 2114−2117.
(35) Colvin, V. L.; Alivisatos, A. P. *J. Chem. Phys.* **1992**, *97*, 730−733.
(36) Colvin, V. L.; Cunningham, K. L.; Alivisatos, A. P. *J. Chem. Phys.* **1994**, *101*, 7122−7138.
(37) Persson, P.; Bergstrom, R.; Lunell, S. *J. Phys. Chem. B* **2000**, *104*, 10 348−10 351.
(38) Stier, W.; Prezhdo, O. V. *J. Phys. Chem. B* **2002**, *106*, 8047−8054.

Table 2. Observed CT Bands and Stark Parameters for Various Mixed-valence Dinuclear Metal Complexes

material	$h\nu_{max,\,77\,K}$ $cm^{-1}\times10^3$	$\lvert\boldsymbol{\mu}_{12}\rvert$ eÅ	$\lvert\Delta\boldsymbol{\mu}_{12}\rvert$ eÅ	$\lvert\Delta\boldsymbol{\mu}_{ab}\rvert$ eÅ	H_{ab} $cm^{-1}\times10^3$	Tr($\Delta\alpha$) Å^3
$(CN)_5Fe^{II}-CN-TiO_2$(particles)[a]	~24	~0.8	~5.3	~5.6	~4.0	~800
$Fe^{II}-Ti^{IV}$cyanide polymer[a]	26.0	0.57	3.6	3.8	3.0	300
$[(CN)_5Fe^{II}-CN-Ru^{III}(NH_3)_5]^-$ [b]	12.2	0.77	2.4	2.9	2.8	230
$[(CN)_5Fe^{II}-CN-Ru^{III}(NH_3)_4py]^-$ [c]	8.3	0.27	4.5	4.8	1.6	1100
$[(CN)_5Fe^{II}-CN-Os^{III}(NH_3)_5]^-$ [d]	17.8	0.44	2.6	2.7	2.5	170
$[(CN)_5Ru^{II}-CN-Ru^{III}(NH_3)_5]^-$ [b]	14.6	0.4	2.8	2.9	3.0	450
$[(CN)_5Ru^{II}-CN-Ru^{III}(NH_3)_4py]^-$ [c]	12.8	0.7	3.8	4.1	2.7	460
$[(CN)_5Ru^{II}-CN-Os^{III}(NH_3)_5]^-$ [e]	NR	NR	3.8	NR	NR	400
$[(CO)_5Cr^{II}-CN-Ru^{III}(NH_3)_5]^{2+}$ [e]	NR	NR	4.5	NR	NR	770

[a] This work. [b] Ref 39. [c] Ref 40. [d] Ref 41. [e] Ref 42 calculated with $f_{int} = 1.33$.

than the geometric separation between the centers.[20] To the best of our knowledge, no cyanide-bridged dinuclear $Fe^{II}-Ti^{IV}$ species has been reported. An approximation of the molecular regime can be obtained by studying the polymeric $Fe^{II}-Ti^{IV}$ cyanide complex.[14,19] The exact structure of this compound is not known, however, it is believed to be similar to Prussian blue. According to Beasley, Milligan and co-workers,[19] the polymer consists of a cubic array of alternating Ti^{IV} and Fe^{II} ions and bridging CN groups on the edges of the cubes, with the estimated $Fe^{II}-CN-Ti^{IV}$ distance of 5 Å. As can be seen from Table 1, compared to the $Fe^{II}(CN)_6^{4-}-TiO_2$(particle) systems, the average Stark-derived charge-transfer distance in the $Fe^{II}-Ti^{IV}$ cyanide complex is significantly shorter than the reported $Fe^{II}-CN-Ti^{IV}$ distance. The polarizability change, Tr($\boldsymbol{\Delta\alpha}$), is also significantly lower for the $Fe^{II}-Ti^{IV}$ complex compared to the particle systems.

It is interesting to compare our findings with the results of Hupp[39−41] and Boxer[42] on a series of cyanide-bridged dinuclear metal complexes (Table 2). For most species the Stark-derived charge-transfer distances were found to be significantly shorter than the geometric metal−metal separation determined by single-crystal X-ray diffraction. However, two compounds, $[(CN)_5Fe^{II}-CN-Ru^{III}(NH_3)_4py]^-$ and $[(CO)_5Cr^{II}-CN-Ru^{III}(NH_3)_5]^{2+}$,[40,42] have significantly larger Stark distances and polarizability changes similar to those in the $Fe^{II}(CN)_6^{4-}-TiO_2$(particle) systems. This suggests that when the polarizability of the excited state increases, larger charge-transfer distances are observed. This could occur when the excited state is much more polarizable than the ground state and the donating center is sufficiently negative that even in the CT state it still appears negative. The negative donating center would polarize both the ground and excited states, but since the polarizability of the excited state is much larger, the effect in the excited state would dominate. The net effect would be to increase the charge-transfer distance. This is the opposite of what is observed for complexes with positively charged donating centers. In the latter case, the increase of positive charge on the donating center causes the excited state to polarize in the direction that reduces the charge-transfer distance.[43]

Conclusions

Electroabsorption spectroscopy was used to study interfacial charge transfer in $Fe^{II}(CN)_6^{4-}$−sensitized TiO_2 nanoparticles. The average CT distance determined from the spectra is close to the minimum iron−titanium separation in the system. The observed charge-transfer distance is longer than that observed in most cyanide-bridged dinuclear metal complexes, and it is attributed to the large polarizability of the excited state in the $Fe^{II}(CN)_6^{4-}-TiO_2$(particle) system. The observed distance, however, is much shorter than one would expect if the electron is transferred to a conduction band orbital delocalized over the nanoparticle. This suggests that the injection occurs to one or a few Ti centers located very close to the point of coordination of the iron cyanide complex.

Acknowledgment. The authors would like to thank Dr. Jonathan Hanson for obtaining X-ray powder diffraction data, Dr. Janet Petroski for help with TEM studies and Dr. Norman Sutin for helpful discussions. The work was supported by the U.S. Department of Energy, Division of Chemical Sciences, under Contract No. DE-AC02-98CH10886.

JA0299607

(39) Vance, F. W.; Karki, L.; Reigle, J. K.; Hupp, J. T.; Ratner, M. A. *J. Phys. Chem. A* **1998**, *102*, 8320−8324.
(40) Vance, F. W.; Slone, R. V.; Stern, C. L.; Hupp, J. T. *Chem. Phys.* **2000**, *253*, 313−322.
(41) Karki, L.; Lu, H. P.; Hupp, J. T. *J. Phys. Chem.* **1996**, *100*, 15 637−15 639.
(42) Bublitz, G. U.; Laidlaw, W. M.; Denning, R. G.; Boxer, S. G. *J. Am. Chem. Soc.* **1998**, *120*, 6068−6075.
(43) Shin, Y.-G. K.; Brunschwig, B. S.; Creutz, C.; Sutin, N. *J. Am. Chem. Soc.* **1995**, *117*, 8668−8669.